Numerical Analysis of Anchoring Effects in Structures

Analyse numérique des effets d'ancrage dans les structures

Nutzung der Betonzugfestigkeit in der Befestigungstechnik

Rolf ELIGEHAUSEN
Prof. Dr.
Univ. Stuttgart
Stuttgart, Germany

Rolf Eligehausen, born 1942, received his Dr. Ing. in 1979 at Univ. of Stuttgart. 1979 – 1981 Research Engineer at Univ. of California at Berkeley. Since 1984 Professor for fastening technology at the Inst. für Werkstoffe im Bauwesen, University Stuttgart.

Mihajlo KAZIC
Res. Eng.
Univ. Stuttgart
Stuttgart, Germany

Mihajlo Kazic, born 1960, obtained his B.S. degree in 1983 in Novi Sad YU, M.S. and Ph.D. in 1986 and 1988 at Univ. of California Los Angeles. Senior Consultant at Pavlovich & Assoc. in L.A. and Teaching Assoc. at UCLA. Since 1989 Research Eng. at IWB, University Stuttgart.

SUMMARY

The shear behaviour of reinforced concrete beams with various types of vertical shear reinforcements and for different load arrangements, modelling the action of headed anchors installed in the tension zone, is numerically analysed by a non-linear finite element program based on a smeared crack approach taking into account non-linear fracture mechanics. Factors affecting the ultimate shear strength are discussed with respect to the numerical analysis and the overall structural response.

RÉSUMÉ

Le modèle mécanique d'affaiblissement de contrainte après fissuration du béton en traction, ainsi que la résistance-même en traction de ce matériau constituent le base du modèle de discrétisation des fissures dans une analyse par éléments finis. Ce concept est ultilisé dans l'analyse du problème du cisaillement de poutres en béton armé sous différentes positions de la charge, celle-ci cheminant dans la matière au moyen des éléments d'armature ancrés dans le béton et les étriers. Les facteurs qui influent sur la résistance ultime à l'effort tranchant sont discutés à la lumière du respect des dispositions énoncées par la Norme au sujet des techniques d'ancrage.

ZUSAMMENFASSUNG

Es wird der Einfluss von durch Kopfbolzen in die Betonzugzone eingeleiteten Lasten auf das Schubtragverhalten von Stahlbetonbalken mit unterschiedlichen Schubbewehrungen untersucht. Die Studien werden mit einem nichtlinearen FE-Programm durchgeführt, das auf dem Konzept der verschmierten Risse unter Berücksichtigung der nichtlinearen Bruchmechanik beruht. Die das Schubtragverhalten beeinflussenden Faktoren werden diskutiert.

1. INTRODUCTION

The shear strength of reinforced concrete beams is almost exclusively studied for the cases where the loads are applied through plates directly onto the top beam surface. However, in modern structures the loads may partly be applied by means of high-tech metal anchoring elements placed in the bottom part of the beam. The influence of this load application by means of anchoring elements on the shear strength of beams without shear reinforcement has been extensively studied by Eligehausen et al. [3]. Their principal conclusion was that on an average the shear failure load is reduced by 10% when the entire load is applied by means of anchoring elements placed in the bottom, tensile zone. The same conclusion was verified by Cervenka et al. [2] in a finite element analysis of reinforced concrete beams with no shear reinforcement.

The present analysis is accomplished by the FE program AXIS, developed at the Institut für Werkstoffe im Bauwesen, University of Stuttgart. The goal was to study the influence of loads introduced into the bottom zone on the shear strength of beams with different vertical shear reinforcements.

2. SCOPE OF ANALYSIS

The analysis concerns reinforced concrete beams failing in shear. The dimensions of the T-beam (Fig. 1) and the shear span ratio $\lambda = a/d = 2.8$ are chosen in order to ensure a shear-tension failure and to avoid a shear-compression (for small λ) and bending failure (for large λ). The principal goal is to investigate the influence of different load arrangements for various stirrups cross-sections on the shear strength. Three different loading cases may be distinguished from Fig. 2, in which load case *a* represents a beam with concentrated loads applied on the top surface. Load case *b* represents the application of 20% of the total loads by means of anchoring elements placed in the bottom zone. Load case *c* is analysed for the sake of direct comparison with load case *b*, with the same shear span ratio and load proportions, but with loads placed on the top surface. Each of this three loading cases was applied on a beam with five different stirrups configurations (no stirrups; two-legged $\phi 6$, $\phi 8$, $\phi 10$ and four-legged $\phi 8$ stirrups, each at a spacing $s = 0.15m$). The longitudinal reinforcement ratio $\rho_w = 2.38\%$ is taken as constant in order to preclude the influence of its variability on the results. Yielding point for all stirrups is $f_{sy} = 350MPa$ and for bending reinforcement $f_y = 450MPa$.

In the bottom part of the web, headed studs with anchoring length $h_v = 100mm$ are located. The stud spacing $s = 0.30m$ is chosen in order to avoid mutual effects of neighbouring studs [3]. The loads applied on the studs are proportional to the loads applied on the top surface, and are smaller than the concrete cone failure load of $55.0kN$ (according to [3]).

Only the effects of static loading are considered. The loads are increased gradually. Load increments are not equal, and depend on the employed arc length iterative procedure, which is a displacement controlled analysis. Effects of repeated, dynamic or reversed loading were not studied.

3. FE ANALYSIS: MATERIAL MODEL

3.1 Concrete Parameters

Reinforced concrete is a highly nonlinear structural material. Prior to crushing or tensile failure, in the FE program AXIS, concrete is considered as a hyperelastic material, for which the stress-strain relations are of the form:

$$\sigma_{ij} = F(I_1, J_2, J_3)\epsilon_{ij} \tag{1}$$

where the initial elastic constants are replaced by scalar functions $F(I_1, J_2, J_3)$ associated with the first invariant I_1 of the stress tensor and the second and third invariants J_2, J_3 of the deviatoric

stress tensor. The nonlinear isotropic elastic stress-strain relation prior to crushing or tensile failure is modelled by a quadratic parabola in compression and by linear loading in tension. A linear strain softening is assumed after crushing and after tensile failure (Fig. 3). The scalar functions $F(I_1, J_2, J_3)$, developed from Kupfer's biaxial experimental data are established to include the variable peak strengths in compression or tension, depending on the total state of stress. The crack is initiated after the principal stress exceeds the tensile strength. The softening modulus in tension E_T is based on nonlinear fracture mechanics and calculated according to the crack band theory of Bazant and Oh [1] :

$$E_T = \frac{E}{1 - \frac{L_{ch}}{L_e}} \qquad L_{ch} = \frac{2G_f E}{f_{ct}^2} \tag{2}$$

in which L_e is the width of an element, or the square root of the area assigned to an integration point. The value L_{ch}, called characteristic length is assumed to be a material property dependant on the fracture energy G_f, modulus of elasticity E and the direct tensile strength f_{ct}.

In the present analysis, the material properties are characterized by only three material parameters, with the following values: uniaxial compressive strength $f_c = 30MPa$, Poisson ratio $\nu = 0.17$ and fracture energy $G_f = 66N/m$. The direct tensile strength f_{ct} is assumed to be a function of the compressive strength:

$$f_{ct} = 0.269 f_c^{0.666} \implies f_{ct} = 0.269(30.0)^{0.666} = 2.60MPa \tag{3}$$

The values of the initial tangent modulus and softening modulus in compression are assumed as:

$$E = 5015\sqrt{f_c} \ \ [MPa] \implies E = 27500MPa \tag{4}$$

$$E_{cc} = -E_c/8.0 \implies E_{cc} = -3500MPa \tag{5}$$

3.2 Shear transfer across the crack

Employing a smeared crack approach, the FE program AXIS has the options for both the fixed crack model based on orthotropic concepts and the rotating crack model based on nonlinear elasticity relations in principal coordinates. In the fixed crack model, the mechanisms of shear transfer accross the crack due to aggregate interlock or dowel action is simulated by reducing the value of the shear modulus corresponding to the crack plane according to the following expression:

$$G = \beta G_{initial} = \beta \frac{E}{2(1+\nu)} \tag{6}$$

In the program, the shear retention factor β can be assumed as constant or variable. For a variable β value the following expression derived by Kolmar [5] is utilised:

$$\beta = -\frac{ln\frac{\epsilon_m}{c_1}}{c_2} \qquad c_1 = 7.0 + 5.0\left(\frac{\mu - 0.005}{0.015}\right) \qquad c_2 = 10.0 - 2.5\left(\frac{\mu - 0.005}{0.015}\right) \tag{7}$$

in which ϵ_m (given in $^o/_{oo}$) is the strain perpendicular to the crack and $\mu \leq 0.02$ is the reinforcement ratio related to the considered finite element.

4. RESULTS OF THE NUMERICAL ANALYSIS

The influence of different crack models on the load displacement behavior of one analysed beam (load case a, stirrups $\phi 10$) is shown in Fig. 4. When using a fixed crack model in connection with variable shear retention factor according to Eq. 7, the beam fails in shear. However, the use of a fixed crack

model with constant shear retention factor, or a rotating crack model will result in a completely different behavior, namely a bending failure with considerably higher ultimate loads. Therefore, the fixed crack model with shear retention factor by Kolmar is used for the entire analysis.

The ultimate stage is reached after extensive diagonal cracking and after yielding of stirrups in case of beams with shear reinforcement. The ultimate shear forces P_u for all analysed cases are listed in Table 1. The ultimate shear stresses, computed by $v_u = P_u/(7bd/8)$, are shown in Fig. 5. A comparison of the results for load case a with empirical formulas by Kordina and Blume [6], Mallèe [7] and Specht [8] is presented in Fig. 6 (see [4] for details). For lower shear reinforcement ratios, the FE analysis gives higher ultimate shear stresses than the empirical formulas. This can be explained by the fact that with the FE analysis a T-beam was considered, while the empirical formulas are valid for beams with rectangular cross section. Test results prove that the shear strength of T-beams is about 20% higher than for beams with rectangular cross-section. Numerically obtained rate of shear strength increase with increasing shear reinforcement ratio ρ_s is somewhat lower than in empirical formulas, but matches well the prediction by the exact truss analogy for which the shear carried by stirrups is equal to: $v_s = \rho_s f_{sy} ctg\alpha$. The angle of major inclined crack α increases (and $ctg\alpha$ decreases) with increasing reinforcement ratios. However, in most code provisions and empirical formulas it is assumed that $v_s = \rho_s f_{sy} K$ in which the constant multiplyer K does not depend on ρ_s. The consequence is a steeper increase of the ultimate shear stress then in the case with $K = ctg\alpha$.

		no stirrups	$\phi 6mm$	$\phi 8mm$	$\phi 10mm$	$2\phi 8mm$
A_s	$[mm^2]$	-	56.5	100.5	157.1	201.1
Load	a	259	291	320	345	384
Case	b	282	308	330	381	428
	c	306	338	375	427	485

Table 1. Ultimate Force P_u (Reaction at the Support) *in* $[kN]$

The values of ultimate shear force in Table 1, and ultimate shear stresses in Fig. 5 reveal higher shear strengths for load cases b and c than for load case a. The reason is a shift from a concentrated load (load case a) towards a more uniformly distributed load (load cases b, c). According to test results, under otherwise constant conditions, the shear strength of a beam with distributed loads is higher than for concentrated loads. This change of loading arrangement represents a change of the shear span ratio and precludes the direct comparison between load case a and load cases b, c.

To study the influence of anchor loads on the shear strength of beams, load cases b and c which have the same shear span ratio are compared. The placement of anchoring elements in the bottom zone (load case b) results in a lower shear strength than for the beam where all loads are applied on the top surface (load case c). The measure of decrease is obtained from a comparison of the ultimate loads by:

$$\Delta P = \frac{P^c - P^b}{P^c} \tag{8}$$

in which superscripts denote load cases. Obtained values are presented in Fig. 7. The results show that the difference of shear strength is within the range of 8 - 11%. The higher shear strength for load case c is explaned in Fig. 8, where from the free body diagram follows that a part of the top load is directly transferred to the support. In contrast to that, the bottom load must be transferred to the top zone by stirrups before being transferred to the support by diagonal struts. Details concerning the decrease of shear strength are discussed in [4]. In the present analysis, the decrease of shear strength for the beam without shear reinforcement is about 8%. This is somewhat higher than found in a similar analysis performed by Cervenka et al. [2] for beams without shear reinforcement where 100% of the load is applied in the bottom zone and a decrease of 8-10% is obtained.

5. CONCLUSIONS

The performed analysis gives an insight into the behavior of reinforced concrete beams which are loaded by a concentrated load on the top surface and by equally distributed loads over the top or bottom zones. The analysis shows that loads introduced into the bottom zone by headed anchors might negatively influence the shear carrying capacity. The effects of different load arrangements are outlined.

References

[1] Bazant, Z. P. and Oh, B. H., "Crack Band Width Theory for Fracture of Concrete", *Materiaux et Constructions*, Vol. 16, 1983, pp.155-177.

[2] Cervenka, V., Pukl, R. and Eligehausen, R., "Computer Simulation of Anchoring Technique in Reinforced Concrete Beams". *Proceedings*, Second International Conference Computer Aided Analysis and Design of Concrete Structures, Zell am See, Austria, April 1990, Pineridge Press.

[3] Eligehausen, R., Fuchs, W., Lotze. D. and Reuter, M., "Befestigungen in der Betonzugzone", *Beton und Stahlbetonbau*, Vol. 84, 1989, pp.27-32. and 71-74.

[4] Kazic, M. and Eligehausen, R., "Numerical Simulation of Shear Problems of Reinforced Concrete Beams", Report in preparation, Institut für Werkstoffe im Bauwesen, Universität Stuttgart, 1990.

[5] Kolmar, W., "Beschreibung der Kraftübertragung über Risse in Nichtlinearen Finite Element Berechnungen von Stahlbetontragwerken", Dissertation, T.H. Darmstadt, 1985, 94 p.

[6] Kordina, K. and Blume, F., "Empirische Zusammenhänge zur Ermittlung der Schubtragfähigkeit stabförmiger Stahlbetonelemente", Deutsche Ausschuss für Stahlbeton, Heft 364, Berlin 1985.

[7] Mallèe, R., "Zum Schubtragverhalten stabförmiger Stahlbetonelemente", Deutsche Ausschuss für Stahlbeton, Heft 323, Berlin 1981.

[8] Specht, M., "Zur Querkraft Tragfähigkeit im Stahlbetonbau", *Beton und Stahlbetonbau*, Vol. 84, 1989, pp.193-198.

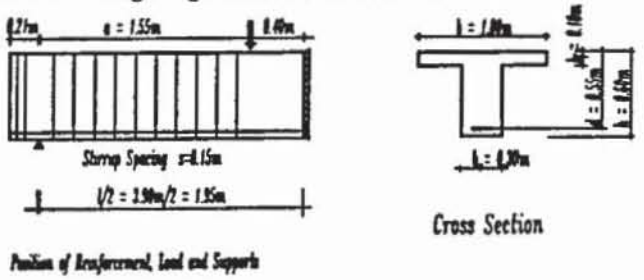

Fig.1 Dimensions of the Analysed Beam

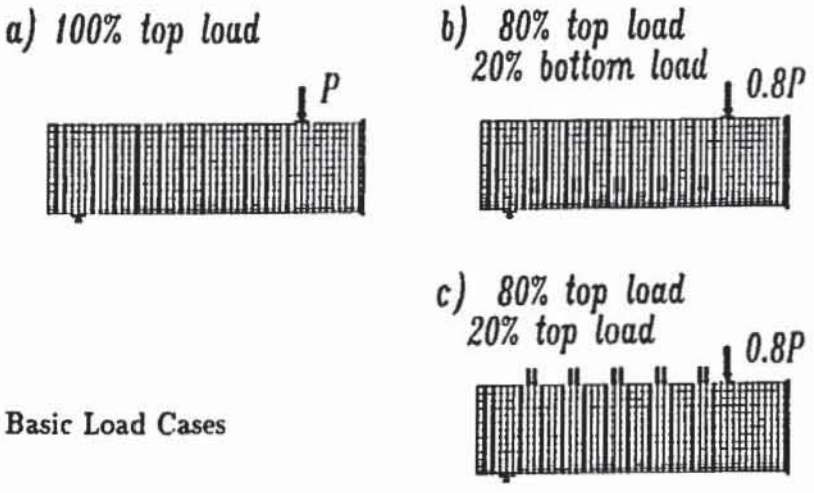

Fig.2 Basic Load Cases

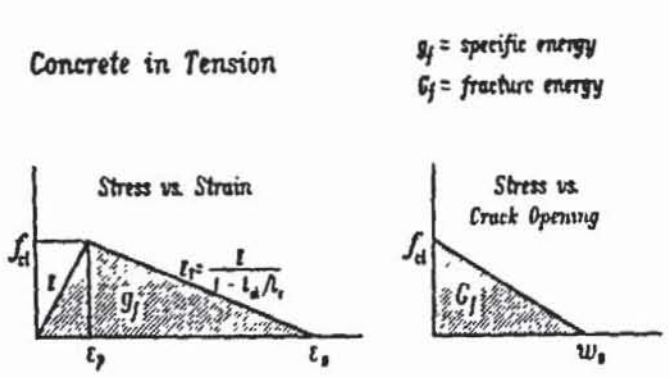

Fig.3 Concrete in Tension

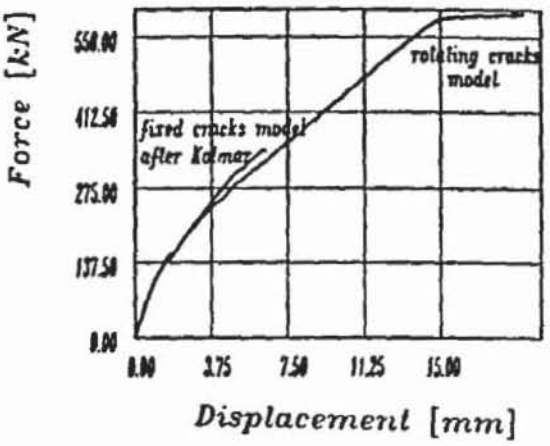

Fig.4 Influence of Crack Model

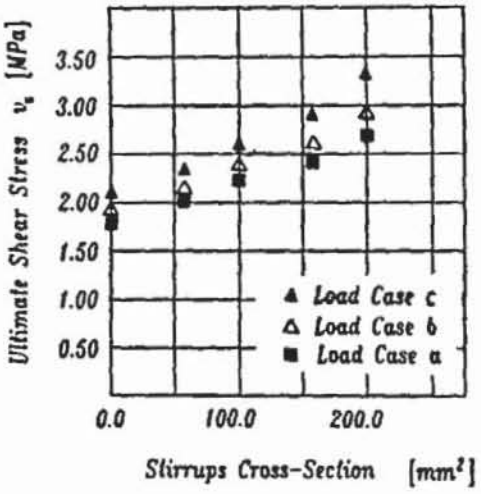

Fig.5 Ultimate Shear Stresses

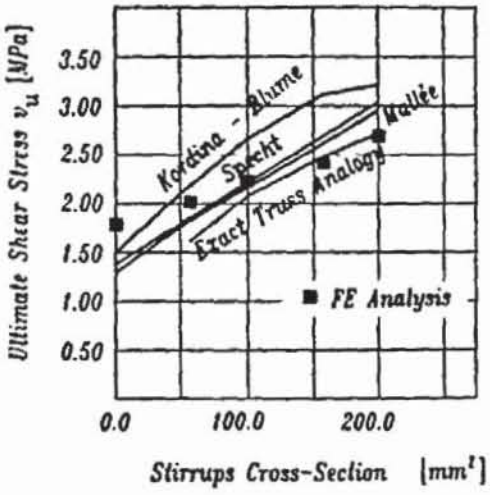

Fig.6 Results vs. Empirical Formulas

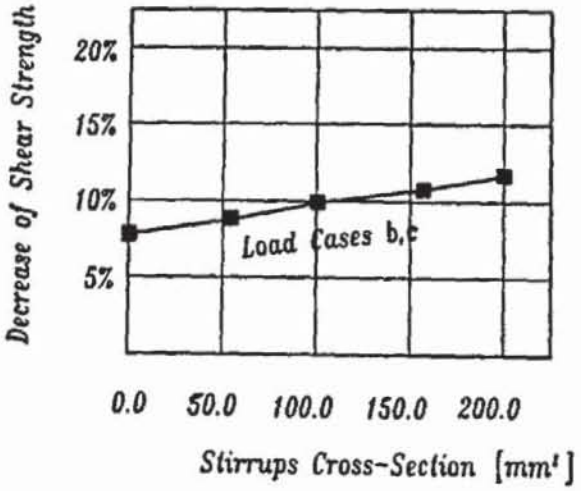

Fig.7 Decrease of Shear Strength

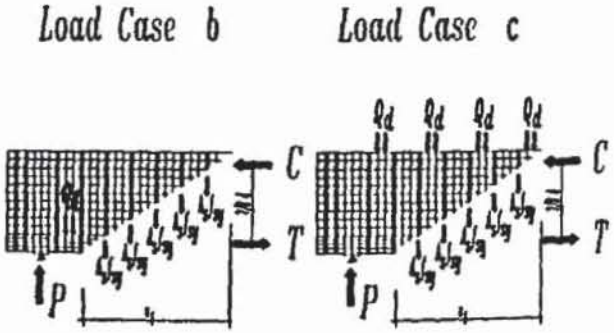

Fig.8 Free Body Diagrams